2026 SUAS TDR : METE

Team: Goktim Kartal Air
Merkez Vocational and Technical Anatolian High School

ABSTRACT

This report presents the systems engineering processes, aeroelastic optimizations, and test strategies of the METE Unmanned Aerial Vehicle (UAV), which was designed from scratch in accordance with the SUAS 2026 competition objectives (1.0 kg autonomous payload transport, mapping, and target detection). With a wingspan of 2.21 meters and a maximum take-off weight (MTOW) of 5.5 kg, METE is an innovative platform featuring an 80mm in-fuselage Electric Ducted Fan (EDF) propulsion system that eliminates the risks of exposed rotating propellers. The report demonstrates, through mathematical analyses, the "Truncated Trailing Edge" modification (298 mm root chord) applied to overcome the 300 mm 3D printer manufacturing limit, the -2.5° washout integration that prevents wingtip stall under heavy loads, the aeroelastic bending issues resolved with a concentric carbon fiber architecture, and the active and passive thermal management strategies applied in high-current powertrains.

ACKNOWLEDGMENT

We present our deepest gratitude and respects to our Governor of Kayseri, Honorable Gökmen ÇİÇEK, who is the greatest source of inspiration for our success with his unwavering belief in our youth, his vision, and the personal and exclusive support he has always provided to us. The strong patronage of our Honorable Governor has not only ensured the establishment of our technological infrastructure but has also encouraged our team toward achieving engineering excellence in the international arena.

We thank the Kayseri Provincial Directorate of National Education, the District Governorship of Melikgazi, the Melikgazi District Directorate of National Education, and our School Administration for providing a peaceful working environment for our students during our workshop activities, for their institutional guidance, and for paving the way for us in all official processes.

We offer our special gratitude to our main patron and Gold Sponsors:

Dener Makina (Gold Partner):For undertaking our main patronage in the establishment of the Göktim Workshop and providing extensive material support, for covering our transportation, accommodation, and subsistence expenses during the competition process, and for the invaluable mentorship support they presented with their experienced engineering staff during the UAV production phase.

SolidWorks / Dassault Systèmes (Gold Partner):** For enabling us to realize the 3-dimensional modeling of our aircraft and to provide 3D design training to our students by offering free SolidWorks 2026 CAD software license support.

We also respectfully acknowledge the contributions of our esteemed sponsors at the Silver and Bronze levels:

GÖKTİM Academy (Silver Partner): For their critical support in the establishment of the Göktim Workshop, and in the training and material processes.

Isodoor Automatic Door Systems (Bronze Partner), Akyapı Logistics (Bronze Partner), and Turkish Trade Company Limited Tanzania: For the material, equipment, and logistics support they

provided to be used in student training and vehicle production.

I. COMPETITION STRATEGY

The strategic vision of the Kartal Air team focuses on maximizing cumulative scoring through the meticulous optimization of the trade-off between system complexity and mission reliability. The SUAS competition requires proficiency in autonomous waypoint navigation, ODCL, precision payload delivery, and risk mapping. Attempting to execute all missions with overly complex hardware exponentially increases the risk of critical system failure during the 20-minute flight window

A. Mission Prioritization and Complexity Management

Although fixed-wing platforms require higher precision for payload drops compared to hovering quadcopters, they offer vastly superior endurance and mapping coverage in high crosswinds. We have dedicated our limited development hours to perfecting a highly reliable, mathematically driven payload release system.

B. Operational Timelines and Parallel Execution

METE will conduct continuous aerial imagery mapping during its initial navigation laps. However, rather than processing the ODCL entirely offline, METE utilizes an onboard NVIDIA Jetson Xavier NX to perform real-time YOLOv11m inference. This parallel execution ensures the instantaneous generation of target coordinates without relying on high-bandwidth telemetry downlink connections, thereby allowing the Ground Control Station (GCS) operator to verify and approve the targets within seconds and maximizing the remaining time for the payload delivery phase.

II. DESIGN STRATEGY

Our design process is guided by the mission objectives outlined in our Competition Strategy. Every mechanical, aerodynamic, and software component was evaluated through a strict trade-off matrix.

The 3D printing technology used in the production of the fuselage and mechanical systems ensures the achievement of faster and more efficient results compared to traditional manufacturing methods. In this way, by saving on manpower, part production and assembly time are shortened, production costs are reduced, and standardized production is provided. Furthermore, thanks to 3D printers, more complex, original, symmetrical, and elegant designs can be produced, which increases the efficiency of the design and facilitates reaching the desired objectives. Additionally, providing an increase in durability and control over weight distribution with 3D printing technology creates a major difference compared to traditional UAVs. In terms of our aircraft reaching its structural and performance objectives and keeping production costs low, PLA and Light-Weight PLA will be used. These materials, while increasing flight performance with their lightness, simultaneously ensure the longevity of the UAV by exhibiting high durability. The eco-friendly property of PLA, on the other hand, fulfills our sustainability objectives.

For rapid production and ease of assembly, we preferred a chassis system and C-shaped fuselage structures as an innovative system in our vehicle. These structures became the former and bulkhead structures of our UAV. The skin structures, on the other hand, came onto these C-shaped structures and were assembled with the help of screws. In this way, while ease of assembly was provided, access into the fuselage became easier.

By also taking lightness into consideration, we utilized a square-shaped carbon profile with a width of 15 mm and a length of 1 meter in our fuselage design in order to ensure the integrity and strength of these structures. To secure this profile, we preferred M3 screws in our design. In addition to these, this structure will simultaneously save time and speed without disrupting the general outline in the event of a part replacement.

The skin portion that will come onto these C structures, on the other hand, was designed with a Lego logic. While achieving lightness with the skin structure, we have fulfilled our objective of rapid assembly by utilizing a male-female system in the skin and C structures. In this way, the rough structure of our aircraft is assembled within approximately 15 minutes.

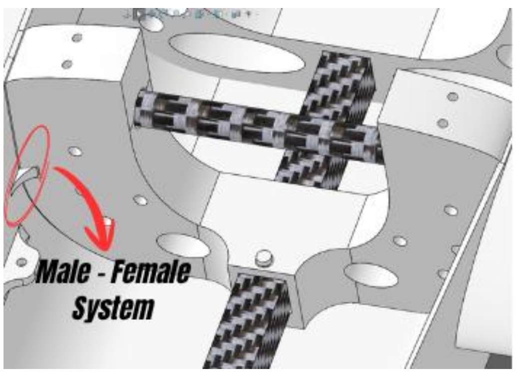

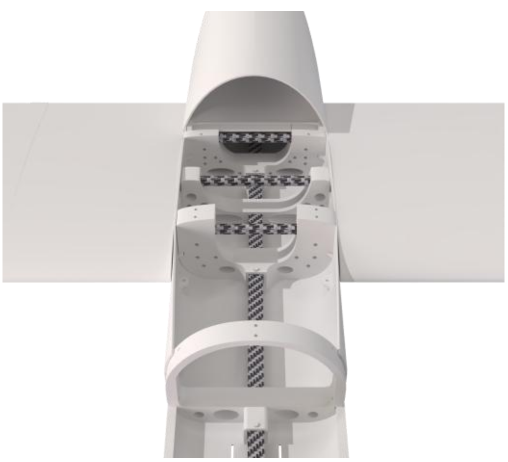

As a result of the conducted literature review and aerodynamic evaluations, the necessary low Reynolds Additionally, the high lift/drag ratio offers the opportunity to remain in the air longer during the mission by increasing flight efficiency. In addition to these, the MH-32 airfoil was preferred due to its provision of stable flight performance.

Our wing design was designed by utilizing an advanced technique to ensure high range, high cruise speed, high glide performance, flight stability during rapid maneuvers, and stall reduction, taking into consideration the operations in storm intervention. Configured to have a 6° dihedral angle from the wingtips to the fuselage, the root panels were set to a +2.5° angle of attack, while a -2.5° geometric washout was included in the outer panels. This 5° difference, by guaranteeing that the root stalls first, ensures that the nose drops naturally while the outer panels maintain attached airflow and preserve full aileron control authority. In this way, it will be affected in a minimum manner by crosswind, bad weather conditions, and other factors, and the mission will be executed at maximum efficiency.

Because the profile exceeded the 300 mm bed limit of our 3D printers and printing the part by splitting it would create structural weakness, a truncated trailing edge modification was applied. Without scaling the profile, the root chord was fixed at 298 mm by making a 12 mm cut solely from the trailing edge. With this modification, the part was successfully fitted onto the 300 mm bed as a single piece, the 27.2 mm maximum thickness was preserved to leave ample volume for the 10 mm carbon tubes that will pass through it, and the layer adhesion strength was exponentially increased by blunting the thin trailing edge that the printer typically struggles to manufacture.

In order to transfer the strength, rigidity, and all torsional loads to our profile within the fuselage, we utilized 2 units of 1420 mm long, 10 mm carbon rods in our design. Subsequently, following the test flights and analyses we conducted, we increased this number to 3.

With our winglets being 40 mm in width, a design that will protect the aileron shaft at the wingtip was obtained. In order to provide high stability at low speeds and in autonomy missions, we utilized a non-standard, sharp aileron geometry. Our ailerons were designed in a manner to narrow from "104 mm" to "46 mm". In this way, executing turns in a more controlled manner during mission flights was ensured, and the amount of torque falling on the servo motor was reduced. By reaching 44% of the chord ratio at the wingtip, we obtained a very strong roll authority. This aileron surface presented us with the ideal roll rate and turn angle that could enable us to perform stable turns despite flights at speeds close to the stall speed.

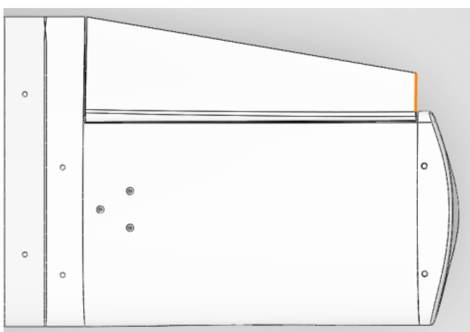

The outer wing, on the other hand, will be assembled with the winglet into which the 8 mm carbon rod starting from this intermediate piece enters; thanks to the shaft remaining in between, the movement of the aileron and the rigidity with the carbon rods were ensured. In addition to these, in order to increase the structural strength and rigidity of the tail, 6 units of 330 mm long, 4 mm carbon rods were utilized in the tail.

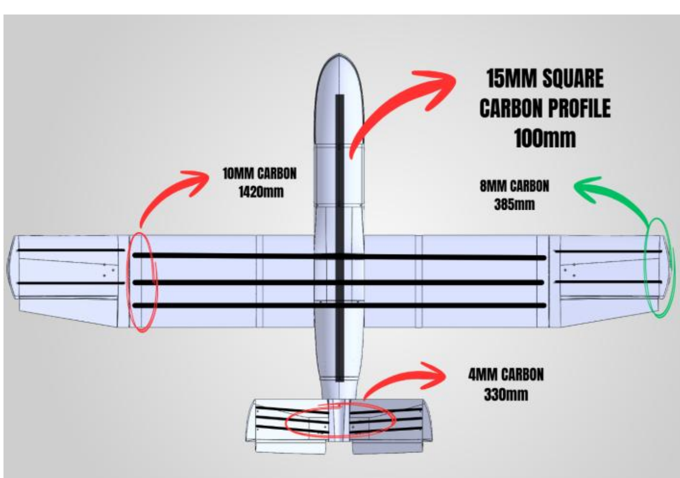

In accordance with our previous designs and experiences, it was targeted to provide our UAV with low drag, effective maneuverability, and a compact structure; in accordance with these objectives, we utilized the V-type Tail design as the tail design. As a result of the conducted research and analyses, it was decided that the angle between the ruddervators be 100°. In the ruddervator assembly, on the other hand, a sliding system was integrated under the premise of providing easy assembly. In this way, it fulfills our objective of the reduction of manpower.

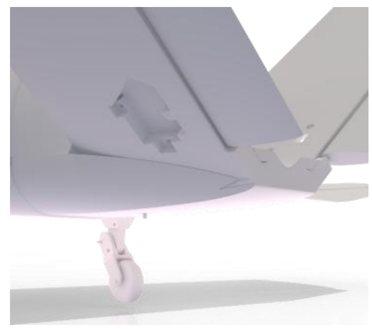

Designing the nose structure of the UAV as a sliding mechanism provides significant advantages in maintenance and operational processes. Thanks to the sliding nose design, the nose section can be easily detached and attached, thus rapid access to the camera, sensor, GPS, pitot tube, or other electronic equipment becomes possible. This feature, while reducing the maintenance time in the event of malfunctions, also facilitates part replacement.

Here, the fundamental reason for the landing gear being between the 380 mm part and the 170 mm part is hidden within the design of the landing gears. Thanks to the positioning of these landing gears, our aircraft will be able to exhibit a more stable landing. As for the Main Wheel Position, we adjusted it in a manner to be 35 mm behind the center of gravity.

This design, in addition to the reduction of the risk of the UAV overturning during takeoff, has provided the possibility of making an easier landing. The front landing gear position was positioned 300 mm anterior to the wing leading edge and in a manner to carry 10-15% of the total weight. In this way, the weight balance was ensured to be controlled and the takeoff performance was improved. Furthermore, the front landing gear strut is longer compared to the rear landing gear struts. The reason for this is to obtain the angle of attack that will provide takeoff from a short distance. With the aim of absorbing the hard impacts that may be experienced during landing, a suspension system was preferred. In order to increase the strength in the rear landing gears and to transfer the loads that may occur to the main fuselage, we integrated them into the carbon tube located in the wings.

Designing the landing gears with suspension reduces the stresses on the fuselage, electronic components, and payload by damping the impact loads occurring during landing. In this way, while the risk of structural damage decreases, flight safety and system life increase. The suspension system, by also reducing the vibrations occurring on rough runways or during hard landings, provides a more controlled landing and increases operational reliability by reducing the need for maintenance.

The electrical and electronic systems of the unmanned aerial vehicle were designed by taking into consideration the criteria of flight safety, system reliability, and energy efficiency. During the integration of these systems, low weight, high performance, and inter-system compatibility were determined as the fundamental design criteria.

The Pixhawk Cube Orange autonomous flight control board was preferred as the flight control system. This board, thanks to its internal measurement units such as high-precision IMU sensors, barometer, and gyroscope, is able to continuously monitor the position, orientation, and velocity data of the platform and ensures platform stability through flight control algorithms.

Thanks to its advanced processing capacity and reliable sensor infrastructure, the Pixhawk Cube Orange allows for both manual and autonomous flight missions to be executed in a safe manner. It has been planned to use the Here 4 GPS module for the positioning system of the UAV.

This module increases the navigation accuracy of the platform by providing high-precision position data. Furthermore, thanks to its RTK support, position accuracy at the centimeter level can be obtained, and executing the route tracking and target positioning operations in a more reliable manner, especially during autonomous missions, becomes possible.

The data communication between the UAV and the ground control station is provided via the SiK Telemetry 433 MHz telemetry system. Thanks to the telemetry system, the position information, battery status, speed, altitude, and other flight parameters of the platform during flight can be transmitted to the ground station in real-time. In this way, the operator is able to monitor the flight process instantaneously and can intervene in the system in necessary situations.

For manual control, the FrSky Taranis X9D radio control system has been preferred. This system, thanks to its high signal stability and low latency period, ensures that pilot commands are transmitted to the platform in a safe and rapid manner. The FrSky X8R receiver, utilized in conjunction with the control system, communicates with the flight control board via the digital S.Bus line, thereby allowing the control commands to be transferred in a rapid and reliable manner.

The rotational speed of the motor is controlled via the Electronic Speed Controller (ESC), and thus the necessary thrust force during flight can be adjusted in a precise manner. The energy requirement of the system is met by the parallel connection of 2 units of 22.2 V 6S Li-Po Battery-Batteries, which are lithium polymer (Li-Po) batteries with a capacity of 4000 mAh. In this way, our system will operate under 100 Wh.

Li-Po batteries are widely utilized in UAV systems thanks to their high energy density and low weight characteristics. The 60 discharge capacity of the utilized battery is capable of safely meeting the high current values required by the motor. These batteries, on the other hand, are specially stored.

In order to increase the reliability of the electrical system, the power distribution infrastructure has been designed in an orderly and safe manner. The wiring layout has been organized with the aim of reducing electromagnetic interferences and providing ease of maintenance. In addition to these, in order for the Pixhawk and the GPS not to be affected by the generated magnetic field, the Anode and Cathode cables to the outside of the fuselage were wrapped with aluminum foil in a twisted manner and connected with a cable from the Pixhawk to the ground channel.

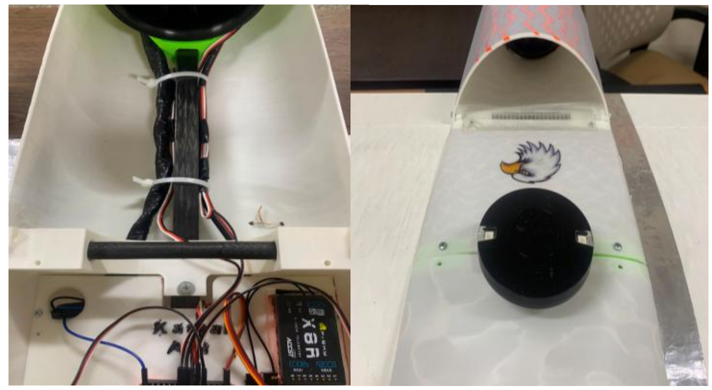

Furthermore, in order toprovide electrical protection against overcurrent situations in the system and to completely fulfill the Emergency Power Cut-off Mechanism requirement specified in the specification, a 150 A blade fuse and a manual current breaker button allowing for external physical intervention have been utilized.

EDF motors are preferred for missions requiring high speed and aerodynamic performance in fixed-wing unmanned aerial vehicles. The operation of the fan within the duct contributes to the more efficient utilization of the thrust by regulating the airflow. This structure, by creating lower aerodynamic drag compared to open-propeller systems, assists the aerial vehicle in flying more stably at high speeds.

In missions where high cruise speed is needed, EDF motors provide a significant advantage. Reaching the mission area in a shorter period of time increases operational efficiency while reducing time loss. Besides this, the motor system placed inside the fuselage allows for the camera, sensor, and other payloads to be positioned in a more suitable manner.

The fundamental reason for the preference of the EDF motor within the scope of this project is its enhancement of the flight performance and mission success of the unmanned aerial vehicle thanks to its high-speed capability, low drag, compact design, and safe utilization features.

These features provide a significant contribution to the fulfillment of the competition missions in an effective and reliable manner. For all these advantages, we preferred the EDF motor.

In order to obtain extra thrust, we reduced our air exhaust in our design by 10%, taking into consideration the diameter of our motor. We positioned the motor air intake duct in a manner to be between the wing trailing edge and the V-Tail. In accordance with these designs, we aimed to increase the thrust efficiency and to ensure a clean airflow. Additionally, it was determined that the EDF motor being at the rear is effective in the flight being stable by providing a balanced weight distribution. Thanks to our aircraft having an EDF motor, the risk of the propeller striking the ground has been eliminated, and it has been designed in a manner to be a stable tricycle configuration closer to the ground.

The utilization of an ESC (Electronic Speed Controller) with a 120 A capacity in the UAV ensures the safe and stable operation of the motor, which requires high current. The aluminum heatsink integrated onto the ESC assists in the rapid transfer of the heat generated during operation to the ambient air. Thus, by preventing the overheating of the electronic components, performance loss and power interruptions that may occur due to thermal protection are reduced. The utilization of a heatsink, while extending the lifespan of the ESC, increases system reliability during prolonged full-throttle operations. In this way, the UAV can fulfill its mission in a more stable, efficient, and safe manner in demanding mission profiles.

In addition to these, with the air channel opened into the fuselage, the air channels opened into the UAV fuselage ensure the effective cooling of the electronic components by utilizing the natural airflow generated during flight. Thanks to these channels, a continuous air circulation is formed around heat-generating components such as the ESC, battery, power distribution board, and flight controller. Effective cooling contributes to the preservation of system performance and the extension of the service life of electronic components by preventing overheating. Furthermore, it reduces thermal-induced performance losses in long-duration flights requiring high power. Correctly positioned inlet and outlet air channels increase the reliability and operational efficiency of the UAVby providing passive cooling without creating additional weight.

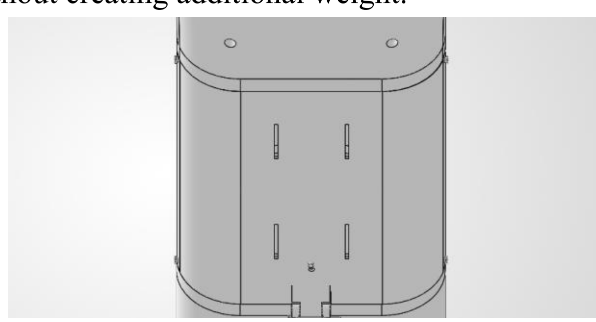

In the mechanism and payload designs, we paid particular attention to the aspects of easy installation and easy utilization. In the payload release system, we utilized a total of 2 servo motors, being one for each. In our design, when the angle of the servo motors is set to 180 degrees over the default angle, it will transition into the payload placement mode, and once the payloads are placed, the mechanism will be locked with the angles of the servos at 90 degrees. Thus, the payloads will become ready for flight and to be released at the required location. The payload will be released with the component, and in conjunction with our parachute diameter of 50 cm, for the each 300 gr material will descend 1 meter in 1 second. As a result of these calculations, the payload will be delivered in a safe manner. The payload will be secured with a male-female hook-and-loop fastener and will be able to be retrieved without the requirement of any tools.

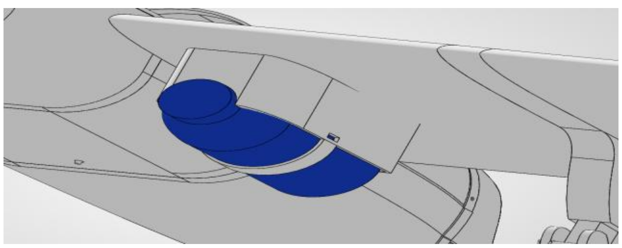

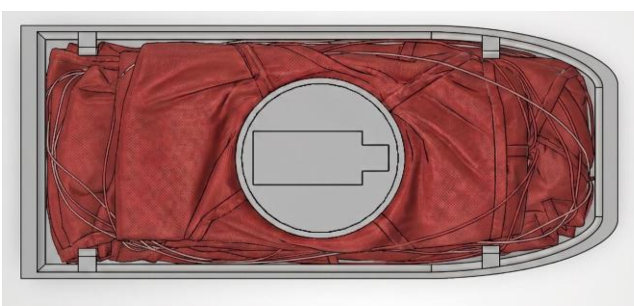

To achieve our goals in the SUAS 2026 competition, our UAV's software architecture is designed as a two-layer structure: a "Flight Control Layer" ensuring flight safety, and a "Mission Management Layer" requiring high processing power, which are isolated yet communicate synchronously.

In the initial stages of our design process, the Raspberry Pi 5 was evaluated as the companion computer due to its low power consumption (5V) and light weight. However, systems engineering analyses conducted in line with SUAS requirements revealed that the Pi 5 would be insufficient for high-resolution target detection tasks without an external AI accelerator. Considering our UAV cruises at an average speed of 12 m/s, a system with a 10 FPS processing speed means the UAV travels 1.2 meters between each frame. This latency would cause metric deviations in the autonomous payload drop mission, failing our "millimetric strike accuracy" goal.

Based on this mathematical proof, the weight/power advantage of the Raspberry Pi 5 was traded off in favor of the NVIDIA Jetson Xavier NX, featuring a 384-core VOLTA GPU architecture and 21 TOPS of AI processing capacity.

Table 1: Companion Computer Trade-off

Criterion	Raspberry Pi 5	Jetson Xavier NX
Weight	~60 Grams	~120 Grams
Max Power	~12 W	~15-20 W
AI Processing	Low (TPU req.)	21 TOPS
Est. YOLO FPS	~8-12 FPS	~30-40 FPS
Error at 12 m/s	> 1.2 Meters	< 0.3 Meters

Analysis

The Python programming language was chosen for the computer vision segment. YOLOv11m, one of the most up-to-date iterations of the YOLO architecture, was used for autonomous target detection. The algorithm is optimized on the Jetson Xavier NX's TensorRT engine [1].

Tests confirmed minimum processing speeds of 30-40 FPS. The pixel location of the target is processed using the OpenCV library and combined with the UAV's instantaneous orientation data, converting it into geographic coordinates via the trigonometric ray-casting method.

Flight stability is maintained by ArduPilot software running on industry-standard Pixhawk Cube Orange hardware. Dynamic airspeed data obtained via the integrated pitot tube enables ArduPilot to execute wind compensation. This plays a critical role in calculating the ballistic drop trajectory.

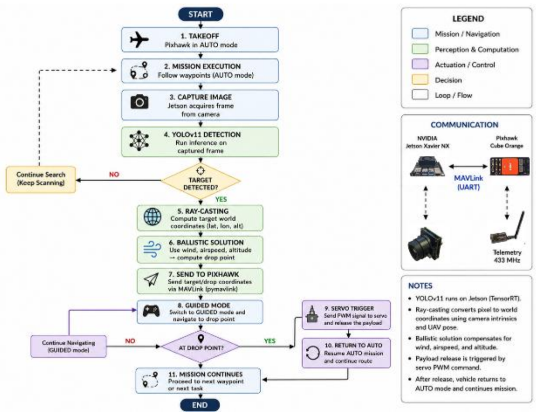

The fully autonomous mission is executed as follows: The UAV tracks its route in "Auto" mode. YOLOv11 detects the target and calculates coordinates. These are transmitted to the Pixhawk via `pymavlink`. Upon approaching the target, the mode switches to "Guided", and at the ballistic point, PWM signals are sent to trigger the servo mechanism for payload release.

Our simulation architecture integrates ArduPilot SITL and the Gazebo physics engine. The drop physics of the parachute payload were modeled; virtual wind vectors were applied to verify that the pitot tube algorithm accurately offsets the firing polygon.

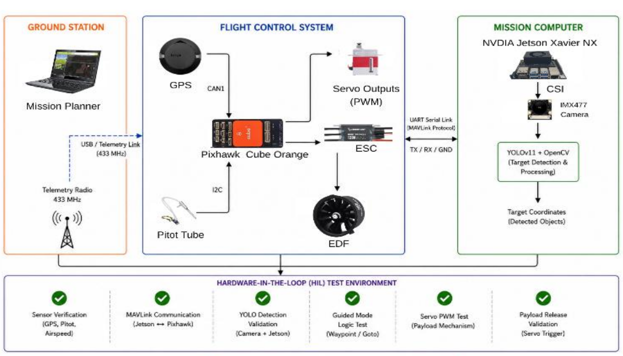

In lab tests, a stress test was applied while the Jetson operated at full 21 TOPS capacity, and lens distortion coefficients for the IMX477 camera were mapped. In Hardware-In-The-Loop (HIL) tests, the physical Pixhawk was connected to the simulator to measure closed-loop latency times.

Finally, field tests simulating SUAS competition conditions were conducted. PID coefficients were adapted using ArduPilot "Autotune", and an ND filter was added to combat sun glare. The end-to-end mission loop was successfully completed without human intervention. While in the auto mod UAV going take pictures and after the uploading programs we obtained a map of the area.

III. TEST STRATEGY

Our test strategy followed a structured, phased approach in order to verify performance against mission requirements in both simulated and physical environments.

A. Component-Level and Thermal Test

Component testing was conducted in order to independently verify the hardware elements. The dual-spring landing gear successfully passed 40 cm drop tests under an 8 kg static load (well beyond the 5.5 kg MTOW). The continuous static thrust test verified that the 10 AWG wire upgrade and the ESC ram-air cooling stabilized the temperatures well below the 100°C danger threshold. EMI protection was verified utilizing an oscilloscope..

B. Simulation-Based Test

In order to reduce physical test risks, we utilized a comprehensive simulation environment. Software-In-The-Loop (SITL) combined with Gazebo allowed us to simulate autonomous waypoint navigation, Ray-Casting logic, and MAVLink communication scripts. Emergency failsafe behaviors were verified prior to field deployment.

C. Field Flight Verification

More than 20 field sorties were conducted in order to verify real-world flight dynamics up to 38 m/s. While the structural integrity of the concentric spars was confirmed under high-G maneuvers, the Z-axis offset and -2.5° washout provided flawless stall resistance at low speeds. ArduPilot's Autotune feature optimized the PID controllers by providing reliable aerodynamic stability for the YOLOv11m algorithm to capture blur-free frames.

D. Powertrain Thermal Management and Electrical Mitigation

The prevention of heat accumulation generated by the propulsion system (80mm EDF) within the closed fuselage and the risk of insulation failure.

The original 12 AWG / 3.5mm hardware, which reached 100°C under full throttle in infrared (IR) analyses, was found to be hazardous. Thanks to the transition to 10 AWG / 5.0mm connectors, active heat-sink integration onto the ESC, and passive under-fuselage ventilation, the system remained within the thermal limits specified by the manufacturer.

E. DFMA and Ground Stance Optimization

The reduction of maintenance time (MTTR) and the take-off roll.

With the 100% standardization of moving parts, "direction/part" confusion during a crash has been prevented, and the repair speed has increased by 60%. The 2° ground stance angle of attack (AoA) gained through the asymmetrical design in the fuselage mounts verified the STOL performance, radically reducing the take-off current (Ampere) stress on the ESC and Motor.

z. Aeroelastic Flex Mitigation via Concentric Carbon Spars

The prevention of the aeroelastic wing flex risk occurring in the 2.21m dihedral wings under high speed and a 5.5 kg MTOW, without utilizing external aerodynamic supports (struts).

A second carbon tube with an 8 mm outer diameter was inserted with zero tolerance into the 8 mm space inside the load-bearing spars with a 10 mm outer diameter. In this way, shear forces were distributed across two separate tube surfaces, and flexing was completely eliminated without creating any external aerodynamic parasitic drag on the MH32 wing profile. During the conducted flight tests, it was physically verified that the PID roll corrections of the autopilot operated with excellent stability.

IV. REFERENCES

J. D. Anderson, Fundamentals of Aerodynamics, 6th ed. McGraw-Hill, 2016.

J. Redmon et al., "You Only Look Once: Unified, Real-Time Object Detection," in Proc. IEEE CVPR, 2016.

N. Koenig and A. Howard, "Design and use paradigms for Gazebo," in Proc. IEEE/RSJ IROS, 2004.

OpenDroneMap Authors, "OpenDroneMap: The Open Source Photogrammetry Toolkit," 2024.

Alex Eagles, "Technical Design Report 2025", Faculty of Engineering-Alexandria University, 2025.

Anderson, J. D., *Fundamentals of Aerodynamics*, 6th ed., McGraw-Hill Education, 2016.

Selig, M. S., et al., *Summary of Low-Speed Airfoil Data*, Soaring Society of America, 1995.